

Spectrum of Magnetic Dissipation and Horizontal Electric Currents in the Solar Photosphere

Valentyna Abramenko

Big Bear Solar Observatory, 40386 N. Shore Lane, Big Bear City, CA 92314

ABSTRACT

A proxy for horizontal electric currents in the solar photosphere was suggested. For a set of evolving active regions (ARs) observed with *Solar and Heliospheric Observatory (SOHO)* Michelson Doppler Imager (MDI) in the high resolution mode, the dissipation spectrum, $k^2 E(k)$, and the spatial structure of dissipation, i.e., the Stokes dissipation function $\varepsilon(x, y)$, were calculated from the observed B_z component of the magnetic field. These functions allowed us to calculate (a part of) the horizontal electric current density in the photosphere. It was shown that as an active region emerges, large-scale horizontal electric currents are gradually generated and determine a bulk of dissipation. When an active region decays, the large-scale horizontal currents decay faster than the small-scale ones. The density of horizontal currents in active regions is in the range of $\langle j_h \rangle \sim (0.008 - 0.028) \text{ A/m}^2$, that is compatible with the density of vertical currents in active regions. We suggest two possible mechanisms for generation of such horizontal currents in the photosphere. One of them is the drift motions of charged particles in the medium of varying plasma pressure gradient in a horizontal plane at the periphery of a sunspot. Such a drift can produce quasi-circular closed horizontal currents around sunspots. Another possibility could be an existence of horizontal axial current inside a highly twisted horizontal magnetic structure laying in the photosphere along the magnetic neutral line. The horizontal currents may contribute significantly to the dynamics of the photosphere/corona coupling, as well as the estimation of non-potentiality of ARs.

Subject headings: Sun: magnetic field; photosphere

1. Introduction

The ultimate source of energy for the majority of non-stationary processes in the solar atmosphere is believed to be a dissipation of the free magnetic energy. This energy,

accumulated via plasma motions, manifests as non-potentiality of the magnetic field or, in other words, as electric currents that permeate through all levels of the solar atmosphere. Electric currents, which can be compared to vortex filaments in a turbulent field, tend to be formed wherever a magnetic field has created a thin layer with both shearing and stretching. Therefore analysis of the electric current evolution seems to be a promising approach to better understand processes of generation and dissipation of the magnetic field as well as accumulation of the free magnetic energy to be released in flares and CMEs.

In spite of the obvious usefulness of information that electric currents could provide, it is not trivial to reliably derive them from observed data. Rare and mostly state-of-art measurements of the vector magnetic field in the photosphere can provide the only vertical component of the current. To derive the horizontal component of the current, vector magnetic field measurements at several heights in the photosphere are required, which are not yet available.

Here we present a new approach to indirectly probe horizontal electric currents. The approach is based on two well known facts, namely, that i) electric current is a product of the magnetic energy dissipation (Moffatt 1978; Parker 1979; Priest 1982) and ii) the magnetic field in the solar photosphere is in a turbulent state (Parker 1979, Petrovay & Szakaly 1993). This allows us to consider the vertical component of the magnetic field, B_z , as a passive scalar in a turbulent flow and thus to analyze its dissipation in the framework of the turbulence theory. Spatial and spectral distributions of the dissipation can then be derived. The former can give us an image of the dissipation over the active region's area, while the later indicates at which spatial scales the dissipation dominates. Physical inferences from such consideration can be made when using the fact that the dissipation of the vertical magnetic field component is intrinsically related to horizontal electric currents.

In Section 2 of this paper we present two approaches (spatial and spectral) to derive the dissipation of the B_z component of the magnetic field and corresponding electric current density. Section 3 is devoted to the application of the technique to emerging and decaying active regions. Discussion is presented in the last section of the paper.

2. Techniques to derive the magnetic dissipation

2.1. Spatial structures of B_z dissipation

Because the B_z component is transported in the photosphere in the same way as a passive scalar does (Parker 1979, Petrovay & Szakaly 1993), one may apply the Stokes dissipation function (Monin & Yaglom 1975) to obtain the spatial structure of dissipation:

$$\varepsilon(x, y) = \frac{1}{2} \left(\left(\frac{dB_z}{dx} \right)^2 + \left(\frac{dB_z}{dy} \right)^2 \right), \quad (1)$$

where (x, y) is a current point on the horizontal plane and z represents direction normal to the solar surface. In general, the right hand part of Eq. (1) requires the magnetic diffusion coefficient, η , which is unknown. Assuming the quasi-uniform behavior of η over the active region area, we will analyze the spatial distribution of dissipation as it is derived from Eq. (1) and measured in G^2/Mm^2 units.

A relationship between the dissipation ε and the squared electric current, \mathbf{j}^2 , can be easily derived from the general formula for the squared curl of the magnetic field vector, $\mathbf{B} \equiv (B_x, B_y, B_z)$:

$$\begin{aligned} \mu^2 \mathbf{j}^2 = (\nabla \times \mathbf{B})^2 = & \left(\frac{dB_z}{dy} - \frac{dB_y}{dz} \right)^2 + \left(\frac{dB_x}{dz} - \frac{dB_z}{dx} \right)^2 + \left(\frac{dB_y}{dx} - \frac{dB_x}{dy} \right)^2 = \\ & \varepsilon(x, y) + \mu^2 j_z^2 + f(B_x, B_y, d/dz). \end{aligned} \quad (2)$$

Thus, dissipation $\varepsilon(x, y)$ represents a part of the horizontal electric current. The spatial structure of $\varepsilon(x, y)$ is shown in Figures 1, 3, and 4. Areas of strong dissipation, and, therefore, strong horizontal currents, tend to be concentrated around strong magnetic elements. Below we discuss the distribution of horizontal currents with possible mechanisms for their formation.

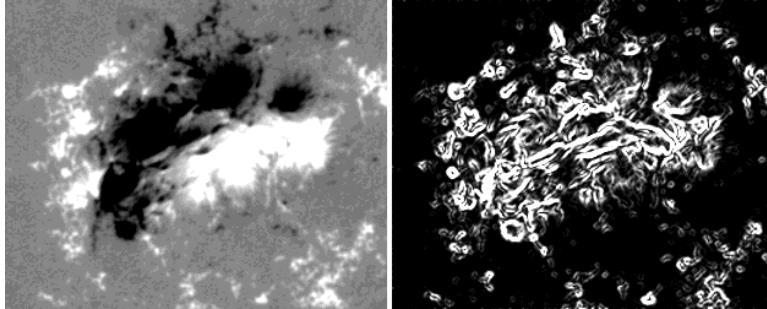


Fig. 1.— MDI/HR magnetograms (*left*) and corresponding dissipation structures, $\varepsilon(x, y)$, calculated for NOAA AR 0365 observed on 2003 May 26/01:01 UT. North is to the top, west is to the right. The image size is 156×126 arcsec. The magnetogram is scaled from -500 G to 500G. The dissipation map is scaled from 0 to $10^5 G^2/Mm^2$.

Averaging $\varepsilon(x, y)$ over the magnetogram area, we obtain the mean value of dissipation $\langle \varepsilon \rangle$ associated with B_z component.

Having the value of $\langle \varepsilon \rangle$ for an active region, we can estimate (a part of) the horizontal electric current by using Eq. (2):

$$\langle \mathbf{j}_h^2 \rangle = \frac{1}{\mu^2} \langle \varepsilon \rangle. \quad (3)$$

Here $\mu = \mu_0 = 4\pi 10^{-7}$ H/m is the vacuum permeability.

2.2. Spectrum of dissipation of B_z

For any measured quantity, which characterizes the photospheric magnetized plasma, one can calculate the spectrum of energy, i.e., a function that shows how the energy (per unit volume) is distributed in the wavenumber space, $k = 2\pi/s$, where s is a spatial scale. The energy spectrum, $E(k)$ (often referred also as a power spectrum), is essentially a squared Fourier transform of a measured array (here we consider a one-dimensional spectrum of a two-dimensional array, see Abramenko (2005) for details of calculation). For a turbulent medium, the energy spectrum displays a maximum at large scales (see Figure 2, blue curve) followed by a power-law decay at smaller scales. The wavenumber where the maximum is reached, marked as k_e (e stands for *energy*), refers to the scales which bear the maximum energy and where the energy input occurs (in our case, this is the largest magnetic elements on a magnetogram).

The spectrum of *dissipation* can be derived from the energy spectrum (Monin & Yaglom 1975) as

$$W(k) = k^2 E(k). \quad (4)$$

Usually, for fully developed turbulence at high magnetic Reynolds number (the ratio of the inertial force to the viscous force), the magnetic dissipation becomes significant at high wavenumbers only. As a result, the maximum of the dissipation spectrum, k_d (see Figure 2), is located at higher wavenumbers than the maximum, k_e , of the energy spectrum. The energy interval (which corresponds to the bulk of energy) and the dissipation interval (which corresponds to the bulk of dissipation) are separated in the wavenumber space: the energy is stored mostly at large spatial scales and dissipated at much smaller scales. The energy cascade is formed from large to small scales, which manifests the presence of the fully developed turbulent state. Turbulent magnetic diffusion seems to be a key mechanism for dissipation in this case.

Sometimes the maximum of dissipation, k_d , is located close to k_e , so that the energy and dissipation intervals are overlapped. In such a case, the dissipation regime differs from the one described above. Namely, the bulk of dissipation occurs at large scales, and both the ohmic dissipation of large-scale currents and the turbulent diffusion at smaller scales

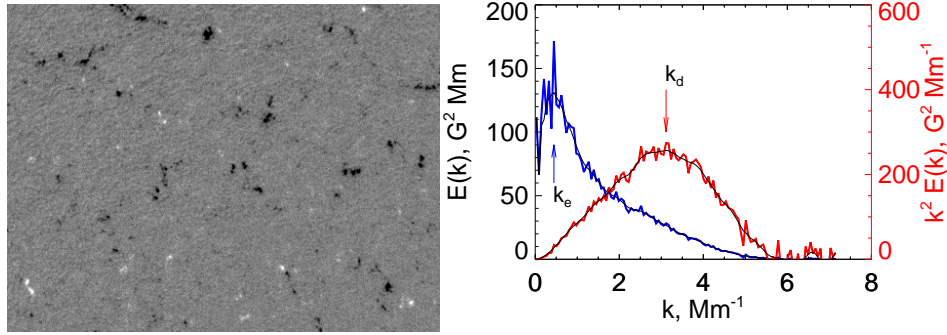


Fig. 2.— MDI/HR magnetograms (*left*) and corresponding energy spectrum, $E(k)$ (*blue curve and right axis*) and dissipation spectrum, $W(k) = k^2 E(k)$ (*red curve, left axis*), calculated for a coronal hole area recorded on 2001 June 5/13:07 UT. Noise influence on the spectra was eliminated. North is to the top, west is to the right. The image size is 266×202 arcsec. The magnetograms are scaled from -150 G to 150G. The arrows k_e and k_d mark the maxima of the $E(k)$ and $W(k)$ spectra, respectively. The locations of the maxima were derived from 5 point box car averaging (*thin curves*). Peaks of $E(k)$ and $W(k)$ are distinctly separated in the wavenumber space.

contribute into the dissipation process. Thus, the dissipation spectrum seems to be useful to diagnose the turbulence and the dissipation regime.

Another advantage of the dissipation spectrum arises from its straightforward relation with the mean squared curl of a field \mathbf{B} (Monin & Yaglom 1975, Biskamp 1993), in other words, with the electric currents:

$$\langle (\nabla \times \mathbf{B})^2 \rangle = 2 \int_0^\infty k^2 E(k) dk. \quad (5)$$

This quantity gives us the mean value of dissipation per unit volume per unit time. We have in our possession the B_z components of the magnetic field only. When we apply Eq. (5) for B_z by substituting the energy spectrum of B_z as $E(k)$, we acquire the part of dissipation associated with the B_z component, i.e., the mean value of dissipation per unit area per unit time measured in units of G^2/Mm^2 . We denoted this value as $\langle W \rangle$:

$$\langle W \rangle = 2 \int_0^\infty k^2 E(k) dk. \quad (6)$$

One can see that $\langle W \rangle$ and $\langle \varepsilon \rangle$ determine the same physical quantity derived, however, from different approaches: from spatial and spectral considerations. This circumstance will allow us to provide two estimations for the mean magnetic energy dissipation. Besides, the

two approaches allow us to study different aspects of the horizontal electric currents. The current density can be derived as

$$\langle \mathbf{j}_h^2 \rangle = \frac{1}{\mu^2} \langle W \rangle. \quad (7)$$

3. Application to active regions

We utilized SOHO/MDI (Scherrer et al. 1995) magnetograms recorded in the high resolution mode. We analyzed areas located at the center of the solar disk (no farther than 15 degree away from the central meridian), so that the projection effect was negligible and the direction of z coincides quite well with the line-of-sight direction.

In this study, we focused on the problem of how the dissipation spectrum and horizontal currents evolve when an active region emerges and decays. An early emergence of an active region can be detected during a 2-day time interval when the magnetic structure is in the close vicinity of the central meridian. We selected three such cases: NOAA ARs 0314, 9574, 0798 (magnetograms and dissipation maps for the last one are shown in Figure 3). However, to detect significant changes at the decay phase, the 2-day interval is rather short. We decided to analyze the decay of a magnetic structure by using observations at two consecutive rotations. For three strong, well-developed active regions: NOAA ARs 9682, 9169, 9165, we determined their remains at the next rotation, namely, NOAA ARs 9712, 9199, 9189, respectively. Magnetograms and dissipation maps for the first pair, NOAA ARs 9682/9712, are presented in Figure 4. As a reference, we also analyzed a coronal hole area shown in Figure 2.

The data for all analyzed magnetograms are compiled in Table 1. The first row refers to a coronal hole magnetogram; three blocks below correspond to three emerging active regions; three pairs below show the data for decaying complexes. The third (fourth) column, r_e (r_d), shows the scale where the maximum of the energy (dissipation) spectrum was located, the fifth column shows the distance between the dissipation and energy maxima in the wavenumber space, $(k_d - k_e)$. The next three columns show the three estimations of the mean value of the magnetic energy dissipation. The sixth column, $\langle \varepsilon \rangle$, is derived by averaging results from Eq. (1) over a magnetogram. The seventh column represents the values W_n calculated from Eq. (6) when noise was not eliminated in calculation of $E(k)$ (for the noise elimination details see Abramenko et al. 2001). The eighth column shows the values W_y calculated from the same Eq. (6), however, noise was preliminary eliminated. Thus, for each magnetogram, we obtained values of $\langle \varepsilon \rangle$, W_n , and W_y , which allowed us to use Eqs. (3, 7) to derive three estimations of the squared horizontal electric current density,

$\langle \mathbf{j}_h^2 \rangle$. The average from the three estimations $(\langle \mathbf{j}_h^2 \rangle)^{1/2}$ is presented in the last column of Table 1.

Table 1: List of studied active regions and calculated parameters

NOAA AR	Data	r_e Mm	r_d Mm	$k_d - k_e$ Mm ⁻¹	$\langle \varepsilon \rangle$ G ² /Mm ²	$\langle W_n \rangle$ G ² /Mm ²	$\langle W_y \rangle$ G ² /Mm ²	$(\langle \mathbf{j}_h^2 \rangle)^{1/2}$ Amper/m ²
CH	2001 Jun05/13:07	14.129	2.018	2.669	3106	3806	1581	0.0059 ± 0.0013
0314 a	2003 Mar13/22:19	18.988	6.995	0.567	6929	6872	4500	0.0087 ± 0.0011
0314 b	2003 Mar14/11:44	44.310	10.223	0.473	20471	19479	16878	0.0155 ± 0.0008
0314 c	2003 Mar15/11:10	44.310	14.766	0.284	35149	33228	30396	0.0204 ± 0.0007
9574 a	2001 Aug10/05:20	31.653	4.996	1.059	12726	12708	10333	0.0122 ± 0.0007
9574 b	2001 Aug10/17:11	31.653	10.547	0.397	39459	38421	37117	0.0220 ± 0.0003
9574 c	2001 Aug11/08:43	31.653	31.653	0.000	58558	60528	59573	0.0275 ± 0.0003
0798 a	2005 Aug18/08:27	47.136	4.873	1.156	6564	6570	4067	0.0085 ± 0.0011
0798 b	2005 Aug18/16:09	47.136	6.729	0.800	9227	8833	6290	0.0101 ± 0.0010
0798 c	2005 Aug19/08:38	47.136	28.264	0.089	13839	12736	10119	0.0124 ± 0.0010
9682	2001 Oct30/17:02	63.853	7.093	0.788	40802	40082	36922	0.0223 ± 0.0006
9712	2001 Nov26/15:46	63.853	2.487	2.428	33839	35281	32545	0.0207 ± 0.0004
9169	2000 Sep23/19:00	86.307	3.547	1.698	59743	59257	55694	0.0271 ± 0.0006
9199	2000 Oct20/20:53	86.307	2.785	2.184	25770	26340	23946	0.0179 ± 0.0004
9165	2000 Sep15/02:00	44.848	3.281	1.775	44853	43850	40661	0.0233 ± 0.0006
9189	2000 Oct12/10:03	26.908	2.862	1.962	15050	15671	14051	0.0137 ± 0.0004

The data from Table 1 show that the coronal hole displays the smallest energy input scales, r_e , as compared to active regions. This can be attributed to smaller typical size of magnetic elements inside coronal holes. A non-trivial inference from the CH data is that the energy dissipation scale, r_d , is smaller and the distance $(k_d - k_e)$ is larger than that for active regions. This implies that in a CH we observe the state of more developed turbulence as compared to ARs. Thus, an assumption of fully developed turbulence seems to be valid for CHs. The current density is smallest for the CH.

Three emerging ARs show a well pronounced trend as the emergence proceeds. Namely, at the very beginning of emergence, we observe the largest distance $(k_d - k_e)$, which resembles the situation in the CH. Later during the emergence this distance decreases by means of shifting of k_d toward the small wavenumbers. The intervals of the energy and dissipation become more and more overlapped (see Figure 5, frames from *a* to *c*) and the current density increases (the last column in Table 1). The observed fact, that during the emergence the bulk of dissipation shifts toward larger scales, implies the formation of large-scale strong currents. In the map of spatial distribution of dissipation (see Figure

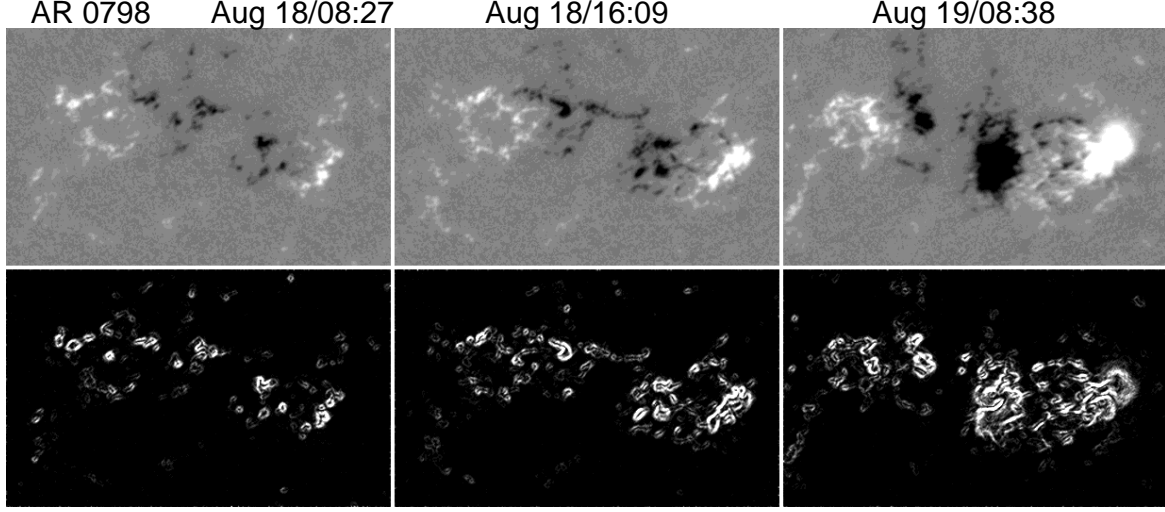


Fig. 3.— MDI/HR magnetograms (*top row*) and corresponding dissipation structures, $\varepsilon(x, y)$, calculated for emerging NOAA AR 0798 (E8 -W15, S10). North is to the top, west is to the right. The image size is 204×126 arcsec. The magnetograms are scaled from -500 G to 500 G. The dissipation maps are scaled from 0 to $6 \times 10^4 \text{ G}^2/\text{Mm}^2$.

3) we see formation of bright contours (frequently closed) surrounding the magnetic flux tubes. Their size increases as the AR emerges.

Three decaying magnetic complexes showed an opposite behavior, see Figure 6. As the magnetic structure decays, the maximum of dissipation shifts toward the smaller scales, large-scale currents decay, the current density decreases and the entire picture begins to resemble what we saw for a CH. Disappearance of large-scale dissipation features is distinctively visible in Figure 4 (compare left and right frames in the bottom row.)

The data obtained allow us to estimate the upper boundary of the plasma conductivity, $\sigma = \tau/l^2$. Here l is a typical scale of decayed current and τ is a typical dissipation time. The data for NOAA ARs 9682/9712 pair show that currents of scales about 7 Mm dissipated during $\tau < 27$ days. This gives us $\sigma < 5 \times 10^{-8} \text{ s/m}^2$, which is four orders of magnitude lower than the classical ohmic conductivity for the photosphere. The magnetic diffusion coefficient in the photospheric plasma of active regions: $\eta = l^2/\tau$ (Priest 1982, here l is a typical scale of decayed magnetic element and τ is a typical decay time). For magnetic elements of 7 Mm dissipated during $\tau < 27$ days we derive $\eta > 2 \times 10^7 \text{ m}^2/\text{s}$, which is four orders of magnitude higher than the classical diffusion coefficient for the photosphere.

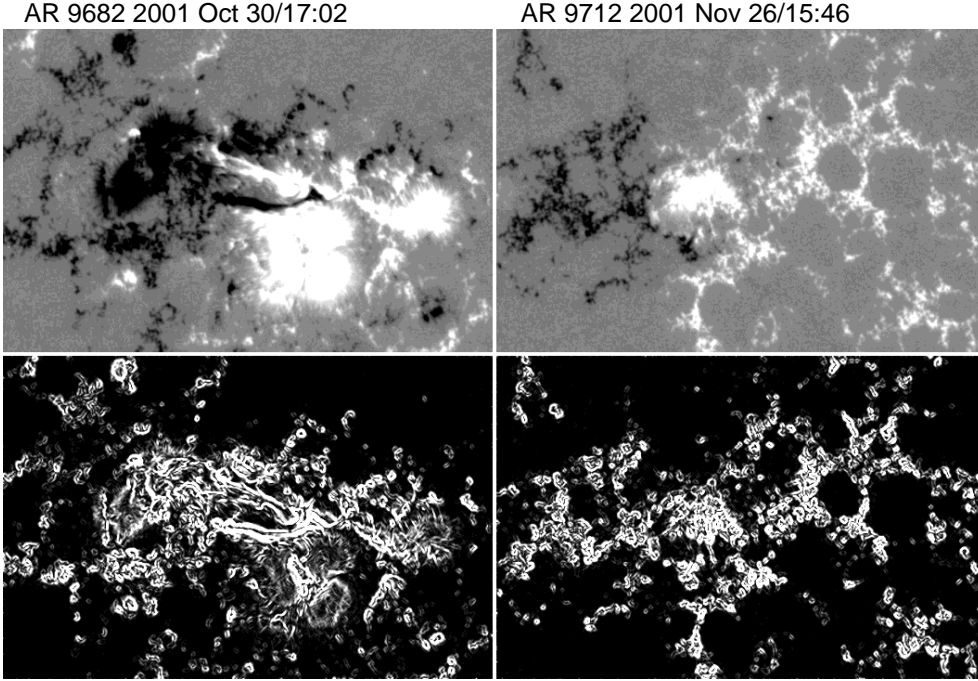


Fig. 4.— MDI/HR magnetograms (*top row*) and corresponding dissipation structures, $\varepsilon(x, y)$, calculated for a decaying complex NOAA AR 9682/9712. North is to the top, west is to the right. The image size is 264×174 arcsec. The magnetograms are scaled from -500 G to 500G. The dissipation maps are scaled from 0 to $9 \times 10^4 \text{ G}^2/\text{Mm}^2$.

4. Discussion

The study presented here suggests that in an active region there exist large-scale horizontal electric currents, which appear and grow during 1-2 days as the AR emerges and slowly decay, during a couple of weeks, when the AR decays. A bulk of magnetic dissipation of the B_z component is associated with these large-scale currents rather than with small-scale currents.

This inference recalls the publications where the photospheric and chromospheric magnetic fields were compared (Abramenko et al. (1992), Choudhary et al. (2002), Leka & Metcalf (2003), Balasubramaniam et al. (2004); see also a recent review by Nagaraju et al. (2008) and references in). Their results suggest that the stronger the line-of-sight magnetic field, the faster it decreases with height. Nagaraju et al. (2008) argued that for the photospheric field stronger than 700 G, the chromospheric field values "are much weaker than what one gets from the linear relationship [between the photospheric and chromospheric fields] and also from those expected from the extrapolation of the

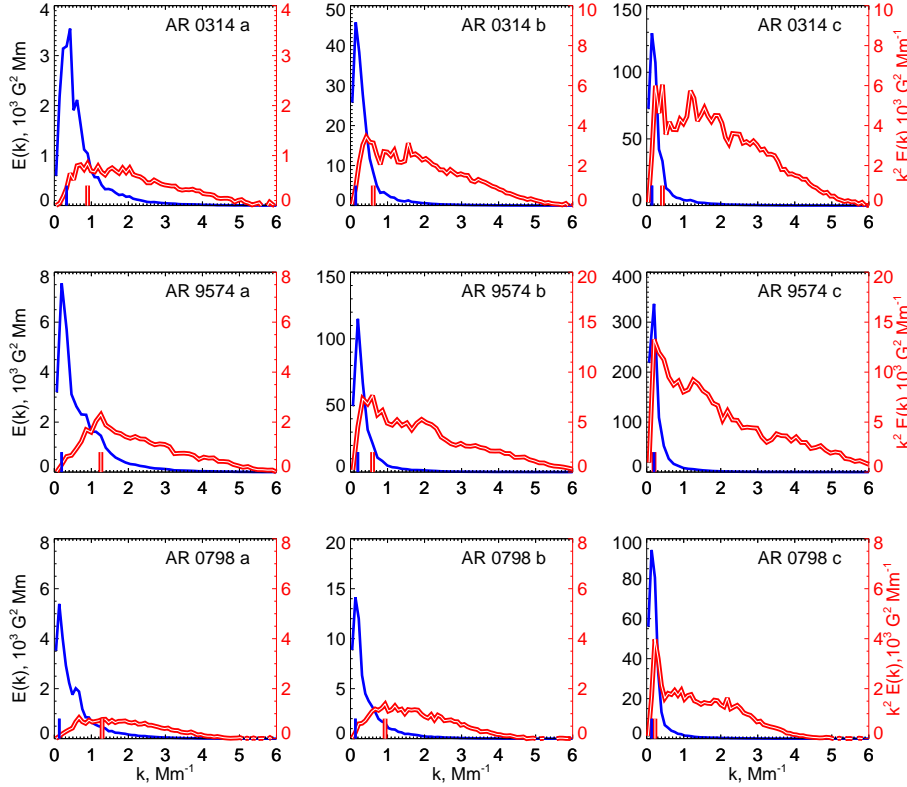


Fig. 5.— Energy spectra, $E(k)$ (blue lines), and dissipation spectra, $k^2 E(k)$ (double red lines), for three emerging active regions. For each AR, frames (a, b, c) correspond to a row with the same mark in Table 1. Vertical blue (red) bars mark the maximum of the energy (dissipation) spectrum. Blue bars correspond to k_e and red bars correspond to k_d . As the active region emerges, k_d shifts toward the smaller wavenumbers.

photospheric magnetic field” in the potential approximation. Leka & Metcalf (2003) observed that the potential field of NOAA 8299 extrapolated from the photosphere to reasonable heights (lower than 2 Mm) statistically exceeds the observed chromospheric field. In 1992 Abramenko and co-authors reported that for NOAA 6280 the chromospheric field measured in H_β spectral line is lower than the extrapolated potential field. They also found that the vertical gradient of the line-of-sight magnetic fields is higher for strong fields. Note, that the above results were obtained from different types of measurements, different spectral lines, different instruments, etc., and still they are consistent with each other.

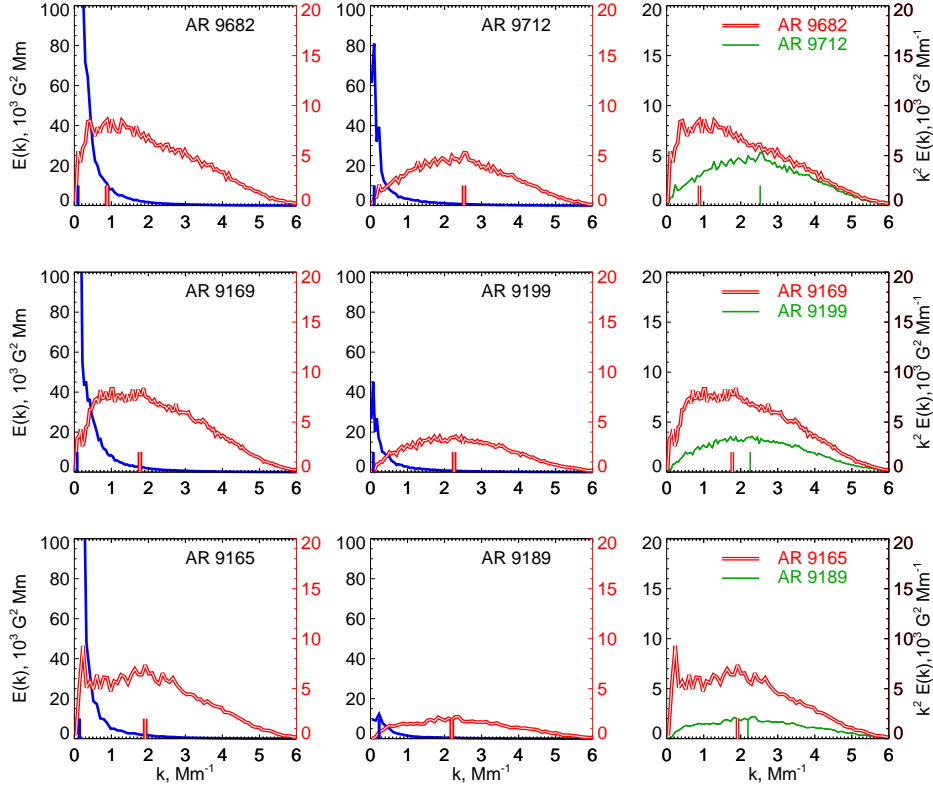


Fig. 6.— Energy spectra, $E(k)$, and dissipation spectra, $k^2 E(k)$, for three decaying magnetic complexes (three rows). The right frame in each row shows a superposition of the dissipation spectra at the well-developed (*double red line*) and decaying (*solid green line*) state of a magnetic complex. As the magnetic complex decays, k_d shifts toward the larger wavenumbers. Other notations are the same as in Figure 5.

Several reasons were suggested to explain the effect (see Nagaraju et al. (2008) for review). However, only one of them addresses the effect of horizontal electric current formation. Namely, in Abramenko et al. (1992) the conclusion was made that the possible reason for such a systematical deviation between the observed and potential fields is the presence of horizontal electric currents enclosing sunspots. The magnetic fields of such currents are predominantly vertical and directed opposite to the original field of a sunspot, so that superposition of the two fields results in the fast weakening with height of the observed field.

We suggest that one of the possible mechanisms for formation of such horizontal currents could be the drift motions of charged particles in the medium of varying plasma pressure gradient in a horizontal plane. Presence of such a medium is unavoidable at the periphery of a sunspot. Such a drift can produce quasi-circular closed horizontal currents around sunspots. This suggestion is in part confirmed by the imaging of the horizontal currents, see Figures 1, 3, 4: in all of them, quasi-circular closed bright structures around sunspots are noticeable.

Another mechanism for the horizontal currents formation can be suggested. Often inside strong active regions with stressed and sheared neutral line one observe strongly elongated magnetic features of both polarities along the neutral line, see, for example, Figures 1, 4. The most obvious way to explain such a phenomenon is to suggest a presence of highly twisted horizontal magnetic structure laying in the photosphere. A strong electric current along the axis of a magnetic helical tube is unavoidably present. A straight long electric current I generates an azimuthal magnetic field B at a distance r from the current axis: $B = 2I/cr$, where B is in Gauss, I in the CGSE system of units, and c is the light velocity. The data for NOAA AR 9682 (see Figure 4) shows that an azimuthal magnetic field of about 500 G is generated at a distance of approximately 3 Mm from the axis of the horizontal current channel laying along the neutral line. This gives us an estimation of the current in the channel as $0.75 \cdot 10^{12}$ A and the density of the current as 0.026 A/m², which is compatible with the magnitude given in Table 1 for this active region.

Emergence of a horizontal helical flux rope along a neutral line was recently reported by Okamoto et al. (2008) from vector magnetic field observations with the Solar Optical Telescope (SOT) on board the *Hinode* satellite.

Taking into account all the above mentioned results, we suggest that strong *horizontal* electric currents are present in the solar atmosphere, and they occupy a large interval of heights: at least, from the photosphere to chromosphere. Their density, $\langle j_h \rangle \sim (0.008 - 0.028)$ A/m², is quit compatible with the density of vertical currents in the photosphere, see, e.g., Abramenko et al. (1991): $\langle j_z \rangle \sim 0.06$ A/m²; Wheatland (2000): $(0.009 - 0.015)$ A/m². The horizontal currents may contribute significantly into the dynamics of the photosphere/corona coupling, as well as into estimation of non-potentiality of ARs. They have to be closely connected with transverse plasma motions, with creation of shear motions. From this standpoint, the recently suggested new approach to study plasma velocities (Nagaraju et al. 2008) seems to be very promising.

One more result of the above study deserves to be briefly discussed. The shifting of the maximum of the dissipation spectrum as an active region emerges and decays indicates that the turbulence regime varies with the evolution of the AR. Namely, as an active region

emerges, the state of fully developed turbulence becomes gradually replaced by a state of under-developed turbulence. The state of under-developed turbulence in mature active regions still bears a signature of a turbulent cascade, that is confirmed by *gradual* decrease of energy along the energy spectrum. High value of the magnetic diffusion coefficient obtained here implies that the turbulent diffusion is significant in well-developed active regions and is responsible to the energy cascading. However, the presence of a bulk of dissipation at large scales suggests that the ohmic dissipation of large-scale currents might compete with the turbulent diffusion in formation of a dissipative regime in the photosphere of well-developed active regions. As the active region decays, the large-scale currents decay faster, as compared to the small-scale currents, and the fully-developed turbulence tends to be restored.

Author is thankful to Prof. Lennard Fisk for a suggestion to use the dissipation spectrum as a proxy for the mean squared curl, to Drs. Vasyl Yurchyshyn, Gregory Fleshman, Haimin Wang for helpful discussions, to Erika Norro and Aaron Coulter for their help with language issues. This work was supported, in part, by NASA NNX07AT16G grant and NSF grant ATM-0716512.

REFERENCES

- Abramenko, V. 2005, ApJ, 629, 1141
- Abramenko, V. I., Gopasiuk, S. I., Ogir', M. B. 1991, Sol. Phys., 134, 287
- Abramenko, V. I., Gopasyuk, S. I., Ogir', M. B., Yurchishin, V. B. 1992, Kinematics Phys. Celest. Bodies, 8, No. 5, 43
- Abramenko, V., Yurchyshyn, V., Wang, H. & Goode, P. R. 2001, Sol. Phys., 201, 225
- Balasubramaniam, K. S.; Christopoulou, E. B.; Uitenbroek, H. 2004, ApJ, 606, 1233
- Biskamp, D. 1993, Nonlinear Magnetohydrodynamics (Cambridge University Press, New York)
- Choudhary, D. P., Suematsu, Y., Ichimoto, K. 2002, Sol. Phys. 209,349
- Leka, K.D.& Metcalf, T.R. 2003, Sol. Phys. 212, 361
- Nagaraju, K., Sankarasubramanian, K. & Rangarajan, K. E. 2008, ApJ, 678, 531
- Moffatt, H.K. 1978, Magnetic Field Generation in Electrically Conducting Fluids (Cambridge University Press, Cambridge, London - New York - Melburn)

- Monin, A.S.& Yaglom, A.M. 1975, Statistical Fluid Mechanics, Vol. 2, ed. J.Lumley (MIT Press, Cambridge, MA)
- Okamoto, T. J., Tsuneta, S., Lites, B. W., and 12 co-authors 2008, ApJ, 673, L215
- Parker, E.N. 1979, Cosmical magnetic fields, their origin and their activity (Oxford University Press)
- Petrovay, K. & Szakaly, G. 1993, Astron. Astrophys., 274, 543
- Priest, E. 1982, Solar Magnetohydrodynamics (Reidel)
- Scherrer, P.H., Bogart, R.S., Bush, R.I., Hoeksema, J.T., Kosovichev, A.G., Schou, J., Rosenberg, W., Springer, L., Tarbell, T.D., Title, A., Wolfson, C.J., Zayer, I. and the MDI engineering team, 1995, Sol. Phys., 162,129
- Wheatland, M.S. 2000, ApJ, 532, 616